IEEE Access
Multidisciplinary ⋮ Rapid Review ⋮ Open Access Journal

Received August 15, 2020, accepted August 30, 2020, date of publication September 3, 2020, date of current version September 18, 2020.

*Digital Object Identifier 10.1109/ACCESS.2020.3021522*

# Size-Invariant Visual Cryptography With Improved Perceptual Quality for Grayscale Image

**RUI SUN, ZHENGXIN FU, AND BIN YU**
Zhengzhou Information Science and Technology Institute, Zhengzhou 450001, China

Corresponding author: Zhengxin Fu (fzx2515@163.com)

This work was supported in part by the National Natural Science Foundation of China under Grant 61602513.

**ABSTRACT** The reconstructed image of the size-invariant visual cryptography (VC) is inevitably accompanied by the loss of secret image information and the degradation of perceptual quality. Here, the halftone technique comes to the forefront since it can realistically simulate the grayscale image from a discrete binary image. Thus, by combining VC sharing with grayscale image halftone technique, this paper proposes a size-invariant VC scheme for grayscale image underpinned by the efficient direct binary search (EDBS) algorithm, in which the multi-pixel encryption VC sharing is adopted into the EDBS halftone process. Through local optimizations and global iterations, the optimal reconstructed image is obtained. To further enhance the contrast of the reconstructed image with limited computational power, the image information is probabilistically extracted according to the inverse mapping in the codebook. It is theoretically proved that the proposed scheme is as secure as the traditional VC, while its effectiveness is validated through experiments and comparative analyses.

**INDEX TERMS** Efficient direct binary search, grayscale image, multi-pixel encryption, perceptual quality, size-invariant, visual cryptography, visual secret sharing.

## I. INTRODUCTION

In 1994, Naor and Shamir [1] introduced the idea of secret sharing into digital images and thus initialized the research on visual cryptography (VC). This approach was different from the traditional cryptography consuming considerable computing resources during decryption. The key characteristics of VC are absolute security and simplicity in reconstructing image. For specific sets of participants, no computational resources but human visual system (HVS) are required to decode the secret image, whereas for the remaining ones, no information regarding the secret image can be leaked. The design of a VC scheme mainly focuses on three aspects, namely reducing pixel expansion, improving perceptual quality, and ensuring security. These aspects are mutually restrictive. In general, security is a hard constraint in the design of a VC scheme.

There exist two approaches for parameter optimization on the premise of ensuring strict security. One is to reduce the pixel expansion toward the pixel-expanded VC schemes [1]–[6], which are collectively referred to as deterministic VC. The deterministic VC schemes can optimize the pixel expansion to some extent but cannot achieve the goal of pixel invariant. With the increasing number of participants, the expansion dilates exponentially, which brings substantial burden for share storage, transmission, and computation; hence, it cannot meet application needs. The other is to improve the perceptual quality of the reconstructed image toward size-invariant VC schemes. The idea of such schemes is to balance the inherent contradiction between the perceptual quality and the size of the reconstructed image by combining the size-invariant VC sharing with the digital image processing method to optimize the perceptual quality of the reconstructed image. This has become the research hotspot of VC, and is also the research objective of this paper.

The main implementation methods of size-invariant VC include the random grid (RG), the probabilistic method and the multi-pixel encryption method. Based on the function operation, Kafri *et al.* [7] proposed a RG scheme and realized the secret image sharing via three functions: randomization, equality, and inversion. The secret image can be revealed by the superposition of sharing images.

The associate editor coordinating the review of this manuscript and approving it for publication was Yizhang Jiang.

On this basis, Chen *et al.* [8] extended the RG to the threshold structure. Concerning to perceptual quality, Wu *et al.* [9] constructed a contrast-enhanced RG scheme and post-processing to obtain an even reconstructed image. Hu *et al.* [10] improved the contrast of $(k, n)$ RG by carefully arranging pixel positions. Wu *et al.* [11] defined the XOR operation for color pixels to generate the color shares.

Ito *et al.* [12] stochastically selected one column from the basis matrices of the deterministic VC to realize a size-invariant scheme. Yang *et al.* [13] formally defined the probabilistic VC, in which the secret pixels are recovered with a certain probability by statistical principles. Hou *et al.* [14] proposed a progressive VC using the elementary matrices to construct the sharing matrices. The quality of shares was promoted, except the reconstructed image. Wu *et al.* [15] utilized colors to generate size-invariant shares, which was inapplicable to grayscale image. The effect of the reconstructed images using the RG is visually similar to that of the probabilistic method. Yang *et al.* [16] proved the equivalence of RG and probabilistic method in theory. Although the perceptual effect of the RG and the probabilistic method was gradually improved, their results could still not achieve a satisfying effect due to independently processing each pixel and disregarding the correlation of pixel distribution in the neighborhood.

As the name suggests, the multi-pixel encryption VC (MEVC) uses multiple pixels as the basic block and maps a secret block into a block containing the same number of pixels in the sharing images, to realize the size-invariant VC. Hou *et al.* [17] proposed an MEVC scheme, in which the basis matrices of the deterministic VC scheme were used as the sharing matrices for the concurrent encryption of $m$ consecutive pixels, while the corresponding sharing matrix was selected by the proportion of black pixels in the secret block. The selection of the basis matrix in [17] was not stochastic when encrypting a block with $i$ black pixels ($i \in [0, m]$). The former $i$ blocks are encoded by $B_1$, and the remaining $m$-$i$ blocks are encoded by $B_0$, which may result in periodic stripes in the reconstructed image. Liu *et al.* [19] optimized the matrix selection approach such that any secret block with $i$ black pixels has a probability of $i/m$ to select matrix $B_1$ and that of $(m - i)/m$ to select matrix $B_0$. The improvement eliminated periodic texture in [17]. Regarding to variable-size secret pixel block, Zhang *et al.* [20] put forward a multi-pixel encryption scheme incorporating deterministic VC and probabilistic VC. However, the selection of sharing methods depending on secret image content may render the shares to leak the contour information, which cannot comply with the security requirement.

Chen *et al.* [21] proposed a scheme to build the multi-level grayscale basis matrices and the block with high average gray value in the halftone image is mapped to the block with high gray value in the reconstructed image. Thus, the reconstructed image obtained stronger representation by profiting from more than two-level grayscale levels. Lee *et al.* [22] selected different mapping combinations leveraging the histogram feature of the grayscale secret image, which inexplicitly realized the histogram equalization and thus improved the visual quality of the reconstructed image.

Halftone VC encodes the secret image into meaningful halftone shares. Zhou *et al.* [23] combined the halftone methods with extended VC sharing to generate good quality halftone shares. In similar, Wang *et al.* [24], Yan *et al.* [25] and Hodeish *et al.* [26] all focused on improving the quality of sharing images. By contrast, Yan *et al.* [27] creatively proposed the AbS framework integrating the error diffusion method and the size-invariant VC to spread the error between the reconstructed and the secret images to a high-frequency band, and generated the reconstructed image with blue noise characteristics.

The problem with the above-given schemes lies in two main aspects. First, most efforts focusing on the grayscale images perform the halftone before VC sharing. The halftone process decreases the information payload and VC sharing reduces the contrast of the reconstructed image. These processes exert a direct influence on the final perceptual effect and separating the halftone from VC sharing is not conducive to realistically simulate the feature information of the secret image. Second, the reconstructed image has low contrast. VC sharing is secure due to randomization, which inherently reduces the contrast and thus greatly affects the visual effect. Besides, the upper limit of the VC contrast optimization is constrained by the basis matrices. Thus, the contrast of the existing solutions has not been effectively improved.

In consideration of these problems, this paper proposes a novel scheme integrating the VC sharing process and the halftone of a grayscale image. Specifically, we combine the MEVC sharing with the efficient direct binary search (EDBS) algorithm to directly optimize the reconstructed image, and achieve realistic simulation of the grayscale secret image. The recovery algorithm follows the traditional VC decryption, i.e., the image reconstruction relies on the superposition of sharing images. For the environment with limited computing power, this paper also designs an information extraction process to obtain a more visually pleasing observation effect. The reconstructed image is probabilistically optimized according to the inverse mapping of the pre-shared codebook; hence, the image contrast is significantly enhanced. In theory, the proposed scheme is as secure as the deterministic VC. The experimental results and the comparative analyses validate the effectiveness of the proposed scheme.

The contributions of this paper can be summarized as follows:

- We propose a structural model combining the MEVC with the EDBS for grayscale image which significantly improves visual quality of the reconstructed image. This model compensates the deficiency of the perceptual effect of the reconstructed image, which not only ensures the unconditional security and simplicity in reconstructing image, but also is effective to improve the perceptual effect.

- We design an information extraction process in which the secret information is probabilistically recovered and the contrast of the reconstructed image is considerably enhanced with limited computational power.

The remainder of this paper is organized as follows: Section II presents the definition of the size-invariant VC for grayscale images and the basic principles of EDBS. In Section III, we propose the structural model and provide the pseudo code. The results of the experiments and comparative analysis are elaborated in Section IV. Finally, we summarize and conclude our work in Section V.

## II. BASIC CONCEPTS

The traditional deterministic VC scheme developed for black-and-white secret image cannot cover the case for grayscale images. Hence, this section first defines the size-invariant VC for grayscale images and then introduces the optimization strategy of EDBS, as well as several image quality evaluation metrics.

### A. DEFINITION OF THE SIZE-INVARIANT VC FOR GRAYSCALE IMAGES

A VC scheme for grayscale image is utilized to encrypt a grayscale secret image and generate $n$ sharing images $S_i \in \mathbb{Z}_2^{M\times N}, i \in [1, n]$ which are then distributed to $n$ participants. Only the specific combinations of participants, i.e., authorized subsets, can decode the information directly by the HVS through overlapping sharing images, whereas the remaining ones, i.e. forbidden subsets, cannot obtain any information about the secret image. For a $(k, n)$ threshold scheme, the authorized subset is a set of all possible combinations with at least $k$ participants. The definition of $(k, n)$ size-invariant VC for grayscale image, $(k, n) - \text{SIGVC}$, is given below.

*Definition 1* $(k, n)$ SIGVC*:* let $B_0 \in \mathbb{Z}_2^{n\times m}$ and $B_1 \in \mathbb{Z}_2^{n\times m}$ be the basis matrices of $(k, n)$ deterministic VC. Blocks $\varphi$ and $\varepsilon$ represent arbitrary two non-overlapping regions with the same number of secret pixels of the grayscale secret image. Without loss of generality, suppose $w(\varphi) > w(\varepsilon)$, where $w(\cdot)$ represents the average grayscale level of the block. Let $v_i^{\varphi}$ and $v_i^{\epsilon}(i \in [1, n])$ be the vector in $n$ sharing images of the corresponding areas $\varphi$ and $\varepsilon$. Let $\mathcal{P} = \{i_1 \ldots i\}$ denote the participant set. Vectors $\varphi'$ and $\varepsilon'$ represent the result of the stacking vector $v_{i_d}^{\varphi}$ and $v_{i_d}^{\epsilon}(i_d \in \mathcal{P})$. If the following two conditions are met, the secret sharing algorithm can be regarded as a valid $(k, n) - \text{SIGVC}$.

1) Contrast condition. For $\lambda \geq k$,

$$\varphi' = V_{i=i_1}^{i_\lambda} v_i^{\varphi}, \quad \varepsilon' = V_{i=i_1}^{i_\lambda} v_i^{\epsilon} \tag{1}$$

satisfies $w(\varphi') \geq w(\varepsilon')$. The symbol $\bigvee$ represents element-wise OR operation.

2) Security condition. For $\lambda < k$,

$$f_\ell = \left[v_{i_1}^{\ell}, \ldots, v_{i_\lambda}^{\ell}\right]^T, \ell = \varphi, \varepsilon, \tag{2}$$

satisfies $f_\varphi \sim f_\varepsilon$, i.e., they have the same statistical characteristics. That is, given the vector $f_l$, one cannot derive any additional information about the secret image.

The first condition guarantees that the secret image can be correctly recovered when there are $k$ participants. It should be noted that $w(\varphi') \geq w(\varepsilon')$, not $w(\varphi') > w(\varepsilon')$. The second condition implies that the result of stacking less than $k$ sharing images would not disclose any information about the secret image.

### B. THE OPTIMIZATION STRATEGY OF THE EDBS

The direct binary search (DBS) [28], a heuristic optimization technology, aims to minimize the visual error between the halftone and the original images by realistically simulating the characteristics of the original image. The global optimization of the DBS algorithm is built upon local optimizations which are realized by the central pixel inversion and eight-neighborhood exchange, as shown in Fig.1, and the transformation result minimizing the local square error is retained. Through the local optimizations and global iterations, the halftone image with a minimum square error is finally obtained.

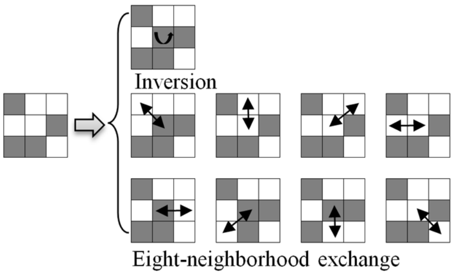

**FIGURE 1.** **The local optimization strategy.**

The specified order of eight-neighborhood scan is as follows:

$$\begin{aligned} Seq &= \begin{bmatrix} -1 & -1 & -1 & 0 & 0 & 1 & 1 & 1 \\ -1 & 0 & 1 & -1 & 1 & -1 & 0 & 1 \end{bmatrix} \\ &= [u_1, \ldots\ldots u_8]. \end{aligned} \tag{3}$$

The HVS is a complex low-pass filter, which can automatically filter out the high-frequency noise components in an image. To maximize the approximation of the original image, the optimization strategy simulates the perception ability of the HVS with vision system model which is mathematically represented by the point spread function (PSF). The original and halftone images are respectively represented as $G$ and $\hat{G}$, and the two-dimensional PSF is denoted as $\mathcal{G}$, and $\otimes$ stands for the convolution. Therefore, we can obtain the following optimization problem:

$$E = min \left\| \mathcal{G} \otimes \left( G - \hat{G} \right) \right\|^2. \tag{4}$$

One of the shortcomings of the DBS algorithm is its high computational complexity occurring due to square error calculation in every inversion/exchange. As the number of iteration increases, the halftone image gradually approximates to the original image, and the number of effective inversion/exchanges of each iteration gradually decreases.

However, the consumption of computing resources does not lessen. Analoui and Allebach [28] introduced the autocorrelation and cross-correlation coefficients into the DBS, which is denoted as the EDBS, to determine the effectiveness of each inversion/exchange by measuring the extent of sensory changes in a specific area. Hence, the calculation of the change quantity is converted into a linear operation. The variation of the local square error, $\Delta E$, can be formulated as:

$$\begin{aligned}\Delta E = &\left(1 + a_1^2\right) c_{\tilde{p}\tilde{p}}\left[0\right] \\ &-2\left(a_0 c_{\tilde{p}\tilde{e}}\left[u_j\right] + a_1 c_{\tilde{p}\tilde{e}}\left[u_i\right] - c_{\tilde{p}\tilde{p}}\left[u_i - u_j\right]\right), \qquad (5)\end{aligned}$$

where $i, j \in [0,8] \& i \neq j$, $u_0$ is the central pixel. The $c_{\tilde{p}\tilde{p}}$ is the autocorrelation coefficient, a constant associated with the PSF, and the $c_{\tilde{p}\tilde{e}}$ is the cross-correlation coefficient updated every time the local optimal value determined. More details can be found in [31].

### C. EVALUATION METRICS

The traditional perceptual evaluation index of the VC is based on relative difference [1], which only works with binary secret image. With the same basis matrices, the global relative difference of the MEVC is the same as that of the probabilistic one. Benefiting from more evenly distributed minority pixels, the former achieves a better perceptual effect. To describe such distinction, Hou *et al.* [18] introduced variance to reflect the smoothness of the local area as well as the relative difference to evaluate the reconstructed image. The variance-based metric is also applicable to binary secret image.

There are three types of objective evaluation methods in digital image processing [32]: non-reference, reduced-reference and full-reference. The non-reference measurement characterizes the features of the image, such as pixel distribution uniformity, dark and light tone. The full-reference measurement describes the similarity between the target and original images, i.e., fidelity. To objectively reflect the visual quality of the reconstructed image, this scheme utilizes radially average power spectral density (RAPSD) as a non-reference evaluation index, while mean structural similarity (MSSIM), and peak signal-to-noise ratio (PSNR) are used as full-reference evaluation indexes.

1) Spectral characterization. The visual rendering quality of a halftone image is closely associated with its frequency domain characteristics, and the distribution of minority pixels in the image can be revealed in the frequency domain. Since the HVS is more sensitive to the low-frequency noise, and the visually-friendly noise model usually has the characteristics of sparse low-frequency energy and concentrated high-frequency energy. In computer graphics, the noise conforming to these characteristics is named as the blue noise. For example, the image generated by the error diffusion halftone technique, whose pixels are evenly distributed, accommodates the typical blue noise characteristics, and thus presents a satisfying visual effect.

The power spectrum density is estimated by the average periodogram, and the halftone process is divided into $K$ overlapping periodograms with a length of each cycle graph being $N$. Hence, the power spectral density can be obtained by:

$$P\left(f\right) = \frac{1}{K}\sum\nolimits_{i=1}^{K} \frac{\left|\mathcal{F}\left\{\emptyset_i\right\}\right|^2}{N}, \qquad (6)$$

where $\emptyset_i (i \in [1,K])$ represents $K$ sample vectors, and $\mathcal{F}$ refers to a two-dimensional Fourier transform. By decomposing the spectral domain and splitting the two-dimensional frequency domain into a series of rings, two easily observable one-dimensional representations: RAPSD $P_p(f_p)$ and anisotropy $A_p(f_p)$ can be obtained. The basic characteristics of a ring are described by the width of the ring $\Delta_f$, the radial frequency $f_p$ on the center radius, and the frequency sample $N_p(f_p)$. The RAPSD can be expressed as:

$$P_p\left(f_p\right) = \frac{1}{N_p(f_p)}\sum\nolimits_{i=1}^{N_p(f_p)} P\left(f\right). \qquad (7)$$

2) Fidelity. For the full-reference evaluation index, the tone and structure similarity of target and original images are measured. The MSSIM [29], an acknowledged measurement standard, considers the combination of local luminance comparison, the local contrast comparison, and the local correlation of two images as one metric. The tonal similarity is often measured by the PSNR. To simulate the intrinsic low-pass filtering characteristics of the HVS [30] and make the calculation results more in line with the perceptual observation, the input signal is processed by the Gaussian low-pass filter with a standard deviation of $\sigma$, and the corresponding indicators are calculated afterward.

## III. CONCEPTUAL DESIGN

In this section, we introduce the design of the EDBS-based size-invariant VC scheme for grayscale image, provide its pseudo-code, and theoretically prove its effectiveness.

### A. STRUCTURAL MODEL

The proposed scheme combines the MEVC sharing with the EDBS to make up for the deficiency of the perceptual effect of the reconstructed image. The access structure is an $(n, n)$ threshold and the algebraic structure is the "OR" operation. Besides, since the color convention of VC is not suitable for combing halftone algorithm and VC, this paper adopts light transmittance to represent the pixel color.

As shown in Fig.2, the model consists of three main parts: the left part implementing the parameter initialization, the right-upper part performing MEVC sharing and the simulated superposition operation, and the right-lower part executing the EDBS algorithm. The operational process of the proposed scheme can be summarized as follows:

- First, generate a stochastic seed image in the initialization part, then partition the seed image with a block of size $b \times b = m$, and then encode the blocks using MEVC and generate $n$ sharing images after quantization.

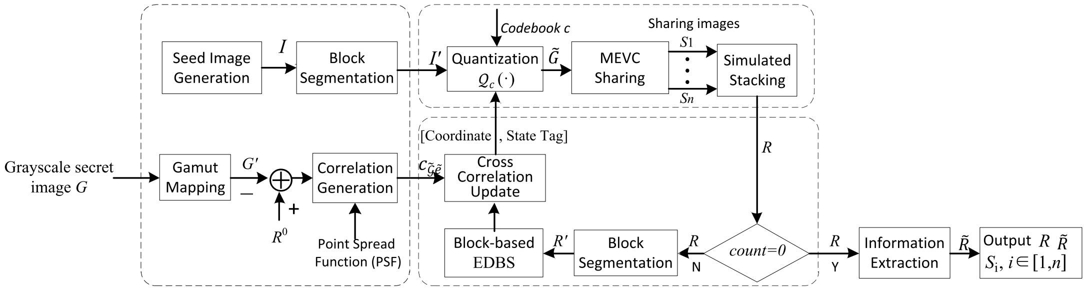

**FIGURE 2.** The structural model of the proposed scheme.

Hence, the reconstructed image $R^0$ which is denoted as $R$ afterward and serves as the optimization objective of the EDBS algorithm, is obtained by superimposing the sharing images.

- Each optimal value is obtained through the block-based EDBS. Then, the MEVC algorithm encodes the optimal value according to Coordinate and State Tag, the coordinate and the color of optimal value, and synchronously updates the sharing images and $R$. It should be noted that we use the reconstructed block rather than the optimal value as the result of each local optimization. With local optimizations and global iterations, the target image $R$ is ultimately determined until there's no changeable value. Ultimately the reconstructed image $R$ and $n$ sharing images are outputted.
- The initial correlation coefficients are produced with $R^0$ at the very beginning of the loop. The cross coefficient updated after each local EDBS optimization acts as the key part to determine whether the current exchange values are valid. The Gaussian model is used as the PSF.

It is assumed that the images can be completely segmented. The goal of this scheme aims to minimize the difference between the reconstructed image $R$ and the secret image $G$, which can be boiled down to the following optimization problem:

$$E = min\,\|\mathcal{G}\otimes(\text{G-R})\|^2. \tag{8}$$

1) Quantization $\mathcal{Q}_c$. The input of the quantization is a binary vector block of size $b\times b = m$, thus the grayscale set is $\zeta = \{0, 1, 2 \ldots .b^2$ with element number of $|\zeta| = b^2 + 1$. Let the set in the reconstructed image be $\psi$. In general, the sets $\zeta$ and $\psi$ have the following inclusion relation $\psi \subset \zeta$, and the mapping $\zeta \to \psi$ is a surjection and non-injection. Thus, more than one element in $\zeta$ are mapped into an element in $\psi$, and the codebook $c$ is utilized to characterize the mapping relationship. It is noted that such a mapping relationship results in the loss of secret information in a size-invariant VC scheme.

2) Gamut mapping. Gamut mapping is to uniform the color space of multiple images performing the linear operation. Since the color space of $R$ is $\psi$, the dynamic range of the grayscale secret image $G$ should be adjusted to match with $\psi$. There are two common methods to realize such conversion, namely linear mapping and non-linear mapping. The former can completely maintain the relative contrast between the grayscale levels of the original image. The latter diffuses or compresses the certain parts of the grayscale level to emphasize or weaken the intensity of some colors. This scheme adopts the linear mapping method to completely simulate the features of the secret image.

3) Block-based EDBS. In this scheme, we take a pixel block of size $b \times b$ as the operation unit. Therefore, the local optimization range is among a $3 \times 3$ pixel-block. The secret pixel block should first be quantified and then the local optimization is performed according to the optimization strategy.

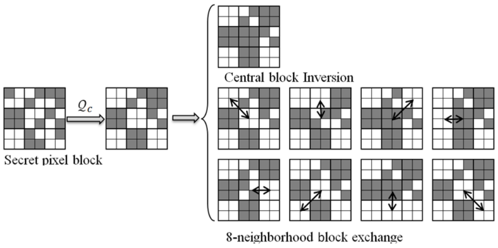

**FIGURE 3.** Block-based local EDBS optimization.

Fig.3 describes the block-based local optimization strategy by taking a $2 \times 2$ block as an example. The block inversion/exchange is used to find the possible optimal solution. Let us assume that the grayscale value of the central block is $M_0$, and each local optimization operation performs the central block inversion and the eight-neighborhood block exchange. The object of central block inversion is the element $\beta \in \psi\{M_0\}$, i.e., all elements in set $\psi$ except $M_0$. Hence, each local optimization needs to calculate the local square error $|\psi| + 8$ times at most, and retain the result of decreasing the local square error most. If there is no such result, the central block is kept unchanged.

4) Information extraction. The information extraction aims to further improve the contrast of the reconstructed image in an environment with limited computational power. For the grayscale set $\zeta = \left\{0, 1, 2 \ldots .b^2\right\}$ of the secret image,

**Algorithm 1** EDBS-Based $(n, n)$ SIGVC

```
Input:   (1) grayscale secret image $G$ of size $M \times N$
         (2) basis matrices $\mathcal{C}_i \in \mathbb{Z}_2^{n\times m}$, $i \in [0, 1]$ of $(n, n)$ VC
         (3) Gaussian filter $\mathcal{G} \in \mathbb{R}^{L\times L}$
         (4) codebook $c$
Output:  sharing images $\mathrm{S_i} \in \mathrm{Z}_2^{M\times N}$, $\mathrm{i} \in [1, n]$, $R \in \mathrm{Z}_2^{M\times N}$,
           $\tilde{R} \in \mathrm{Z}_2^{M\times N}$
Step 1.  initialize parameters
Step 2.  encode $I$' using the MEVC and simulated stacking
           to obtain $R^0$
Step 3.  generate the cross-correlation:
           $e = R^0 - G', (e, c_{\tilde{\mathcal{G}}\tilde{\mathcal{G}}}) \xrightarrow{yields} c_{\tilde{G}\tilde{e}}$
Step 4.  for every block of size $b \times b$ in $R$
Step 5.  apply the EDBS to search for local optimal
           value and update $c_{\tilde{p}\tilde{e}}$
Step 6.  encode the changed block using MEVC, update $\mathrm{S}_i$
           and $R$
Step 7.  if $count$ =0, turn to Step8; else, turn to Step 4
Step 8.  loop termination, output $S_i$ and $R$
Step 9.  calculate the mean grayscale value $T$ of the pixel
           block of size $b \times b$
Step 10. for every block $B$ in image $R$ of size $b \times b$
Step 12. if $\varpi(B) > T$, replace it with $a = (a \in \zeta_1 \& p(a) p_1)$
Step 13. else, replace it with $a = (a \in \zeta_2 \& p(a) p_2)$
Step 14. output the optimized image $\tilde{R}$
```

the block is mapped into a grayscale level set $\psi$ according to the codebook. The information extraction is the inverse process.

The mapping from $\psi$ to $\zeta$ is also a surjection and non-injection, where an element in $\psi$ may correspond to multiple elements in $\zeta$. Assuming that $\psi = \{g_1, \cdots g_t\}$, the mapping relationship between $\psi$ and $\zeta$ is shown in Fig.4 where the element in $\zeta_i$ is recovered with the probability of $1/|\zeta_i|, (i \in [1, t])$.

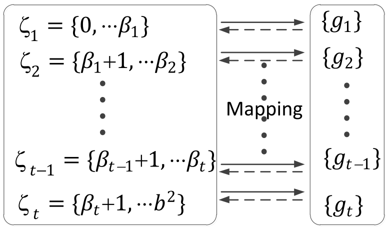
$\zeta_1 = \{0, \cdots\beta_1\}$
$\zeta_2 = \{\beta_1+1, \cdots\beta_2\}$
$\zeta_{t-1} = \{\beta_{t-1}+1, \cdots\beta_t\}$
$\zeta_t = \{\beta_t+1, \cdots b^2\}$
Mapping
$\{g_1\}$
$\{g_2\}$
$\{g_{t-1}\}$
$\{g_t\}$

**FIGURE 4.** **Mapping relationship.**

Our scheme adopts the two-level grayscale, i.e., $|\psi| = 2$. Now, suppose that $\psi = \{g_1, g_2\}$, and the elements in subset $\zeta_1 = \{0, 1, 2 \ldots \beta\}$ are mapped into $g_1$, and the elements in subset $\zeta_2 = \{\beta + 1, \ldots .b^2\}$ are mapped into $g_2$. Hence, the element in $\zeta_1$ is revealed with the probability of $p_1 = 1/|\zeta_1|$ at the grayscale level $g_1$, and thus $p_2 = 1/|\zeta_2|$ for $g_2$. The corresponding pseudo-code is given in *Algorithm*.

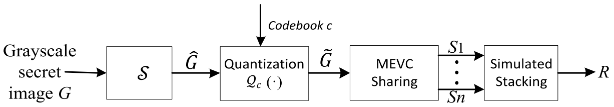

**FIGURE 5.** **The abstracted diagram of the structural model.**

### B. PROOF OF VALIDITY

To facilitate an understanding and expression, the structural model is abstracted as in Fig.5, where $\mathcal{S}$ represents the EDBS algorithm, and $\hat{G}$ denotes the halftone image corresponding to the reconstructed image $R$, i.e., $\hat{G} = \mathcal{S}(G)$. Let a vector $\mathscr{z}$ in $G$ denote as $\hat{\mathscr{z}}$ in $\hat{G}$, $\tilde{\mathscr{z}}$ in $\tilde{G}$, and $\mathscr{z}'$ in $R$.

*Lemma 1 [19]:* For a $(k, n)$ MEVC scheme for a binary secret image, two secret blocks, $x$ and $y$ of the same size are denoted as $x'$ and $y'$ in the reconstructed image. For the number of participants $\lambda \geq k$, if $\varpi(x) > \varpi(\mathrm{y})$, then $\varpi(x') > \varpi(y')$.

*Theorem 1:* The proposed EDBS-based $(n, n)$ SIGVC scheme meets the contrast requirement.

*Proof:* The average grayscale of a block in $G \rightarrow \hat{G} \rightarrow \tilde{G}$ possesses a chain reaction. Suppose that $\varphi$ and $\varepsilon$ are two un-overlapped blocks with the same size in the secret image $G$. If $\varpi(\varphi) > \varpi(\varepsilon)$, then $\varpi(\hat{\varphi}) \geq \varpi\left(\hat{\varepsilon}\right)$ and $\varpi(\tilde{\varphi}) \geq \varpi(\tilde{\varepsilon})$. According to Lemma 1, $\varpi(\varphi') \geq \varpi(\varepsilon')$ holds.

*Theorem 2:* The proposed EDBS-based $(n, n)$ SIGVC scheme meets the security requirement.

*Proof:* For $\lambda < n$, suppose that $PB_1$ and $PB_0$ stand for the collection of all possible column permutation by restricting $\lambda$ rows of matrices $B_1$ and $B_0$. Each block in $\tilde{G}$ are encoded by the matrices in $PB_1$ and $PB_0$. According to the security condition in [1], $PB_1$ and $PB_0$ have the same sample space and the probability distribution. In other terms, these two collections are the same; thus, $f_\varphi \sim f_\varepsilon$, and $= \varpi\left(\varphi'\right) \varpi(\varepsilon')$ holds.

It can be observed that the effectiveness of the proposed scheme is equivalent to that of the Naor-Shamir VC [1].

## IV. EXPERIMENTS AND RESULT ANALYSIS

In this section, first the effectiveness of the proposed scheme is validated through experiments. Then, we analyze the perceptual quality and fidelity of the reconstructed image and compare it with typical size-invariant VC schemes. Finally, the computational complexity is analyzed.

To ensure the persuasiveness of comparisons, the following conditions have to be met: i) reference algorithms strictly abide the security condition of VC; ii) the encryption object is a grayscale image; iii) the algebraic structure is an "OR" operation; iv) the content of comparison is the perceptual quality of the reconstructed image. Based on the above conditions, we pick Yang *et al.* (2004) [13], Liu *et al.*'s (2011) [19] Construction III and Yan *et al.* (2019) [27] as comparative references. Among them, [19] is the improved version of Hou *et al.* (2004) [17], hence we do not compare with [17] anymore. Construction IV of [19] is based on weak security condition, thus no comparison is made either. Besides, multi-level VC is applied in [27], so we no longer consider Chen *et al.* (2007) [21] and Lee *et al.* (2014) [22].

### A. VALIDATION

We use the grayscale image Lena of size 512 × 512 from the standard image dataset to validate the effectiveness. The pixel block is of size 2 × 2, and the basis matrices are as follows:

$$\mathrm{B}_0 = \begin{bmatrix} 1\,0\,1\,0 \\ 1\,0\,1\,0 \end{bmatrix}, \quad \mathrm{B}_1 = \begin{bmatrix} 1\,0\,1\,0 \\ 0\,1\,0\,1 \end{bmatrix}. \tag{9}$$

Fig.6a is the grayscale secret image, while Fig.6b and Fig.6c are the two sharing images generated out of it. Any sharing image is a noise-like image with evenly distributed black and white pixels. The shares do not reveal any information about the secret image, which satisfies the security condition. Fig.6d is the reconstructed image obtained by superposing the two shares together, which satisfies the contrast condition. The structure is realistically revealed in Fig.6d, and the textures are also clearly displayed. In terms of hue, the contrast of the reconstructed image is evident between the light and dark areas. Apart from maintaining the structure of Fig.6d, the optimized image in Fig.6e, greatly enhances the contrast. Since the inverse mapping extracts information with a certain probability, the similar bright areas are recovered with the elements in the same subset, which leads to the unevenly distributed minority pixels. These results verify the effectiveness and feasibility of the proposed scheme.

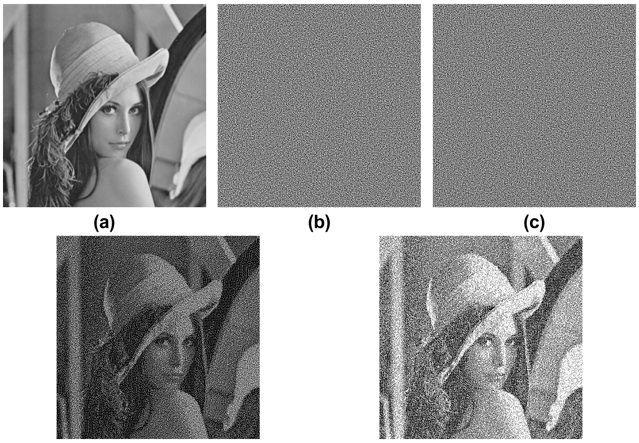

**FIGURE 6.** The experimental results obtained with Lena.

### B. IMAGE QUALITY ANALYSIS

For the quality analysis of the constant images, we select four representative grayscale values and perform perceptual observation, RAPSD spectrum analysis and average grayscale comparison to assess the pros and cons of each scheme. The sample set of the constant grayscale images of size 512 × 512 is $\mathcal{J} = \{51, 119, 153, 221\}$.

**TABLE 1.** The Reconstructed Images of the Constant Images.

| Constant images<br>Schemes | <br>$J$=51 | 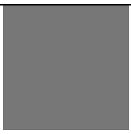<br>$J$=119 | 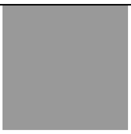<br>$J$=153 | 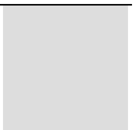<br>$J$=221 |
|---|---|---|---|---|
| Yang *et al.* [13] | 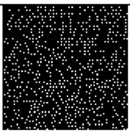 | 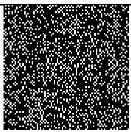 | 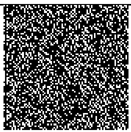 | 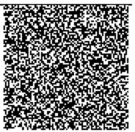 |
| Liu *et al.* [19] | 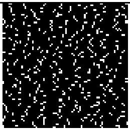 | 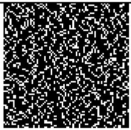 | 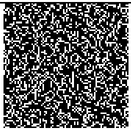 | 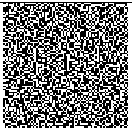 |
| Yan *et al.* [27] | 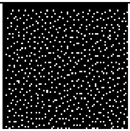 | 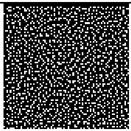 | 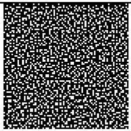 | 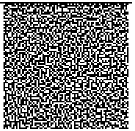 |
| This scheme | 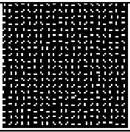 | 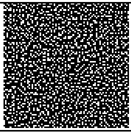 | 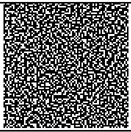 | 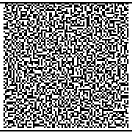 |

Table 1 shows the reconstructed images of different constant images. To ensure fairness, the optimized image of this scheme is beyond the scope of comparison. Besides, to avoid image distortion caused by scaling, the results shown in Table 1 are the originals intercepted by 70 pixels vertically and horizontally. The halftone images with the error diffusion method are utilized as the encoded object in both Yang *et al.*'s and Hou *et al.*'s algorithms. The overall pixel distribution of the former is more uniform than the latter for low grayscale levels. With the increase of the grayscale value, more black pixels turn into white, and the minority pixels are enriched locally, which deteriorates the perceptual quality. Yan *et al.*'s algorithm diffuses the error between the reconstructed and the secret images to its neighborhood blocks. Hence, the deterioration in perceptual quality caused by the aggregation of the minority pixels is effectively alleviated. In doing so, the visual quality is significantly improved compared to Hou *et al.*'s algorithm.

In this scheme, when the grayscale level is low, there occurs the phenomenon of local concentration and global even distribution of minority pixels due to block-by-block sharing. The first image shows a grid-like pattern, which can lead to a high energy density at certain frequencies. With the increase of the grayscale level, the number of white pixels also increases, which weakens the impact of the block-based sharing. The perceptual quality of the reconstructed image does not deteriorate with the increase of the grayscale value.

The results of the proposed scheme are visually friendly and consistent with the characteristics of the blue noise. In terms of hue, the brightness of each grayscale level is perceptually higher than that of Yan *et al*'s scheme. This phenomenon can be interpreted by the different principles of the EDBS and the error diffusion. The central block performs flipping during local optimization, which makes an adaptive adjustment with the tone of the secret image. This mechanism can realistically simulate the original image and improve the contrast of the reconstructed image.

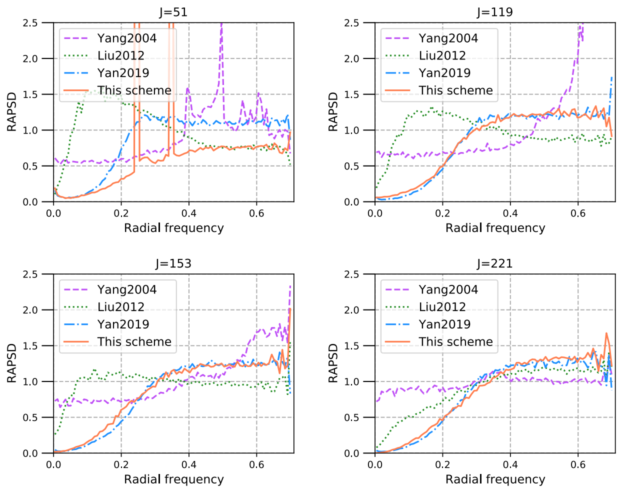

**FIGURE 7. Comparison of the RAPSD.**

From the visual point of view, we make a qualitative analysis on the constant image. Subsequently, from the frequency domain point of view, the performance of the reconstructed images is exhibited more intuitively. Fig.7 is the PAPSD diagram of Table 1 for the four grayscale values. Compared to other schemes, Liu *et al.* produce the most concentrated low-frequency energy at low grayscale values, which is in line with the poor perceptual observation effect in Table 1. The low-frequency energy gradually declines with the increasing grayscale values. Yang *et al.*'s scheme is with flat but high energy on the low-frequency band for all grayscale values.

The oscillogram of the proposed scheme is similar to that of Yan *et al.*'s in the wave trend, which shows obvious blue noise characteristics and good graphic property. When the grayscale value is 51, there is a steep pulse signal in the frequency map, which indicates that the energy density is mostly concentrated in these frequencies. It is easy to associate such phenomenon with the grid-like graphic features in the reconstructed image. Similar local areas produce similar spectral powers and lead to power focus at certain frequencies. Regarding the above analysis, the visual observation in Table 1 and the RAPSD oscillogram in Fig.7 validate each other, and demonstrate the good performance of the proposed scheme.

The brightness of the image reconstructed by the proposed scheme is visually higher than that of the reference schemes. We verify the conjecture by comparing the average grayscale values. As shown in Fig.8, the diamond-shaped dashed line is the grayscale value, $\mathcal{J} = \{g|g = 17 \times i, i \in [0, 15]\}$, of the constant image. For the (2, 2) threshold, the contrast of the reconstructed image normally declines by half, i.e., the average grayscale value of the reconstructed image is half of the constant image. As seen, the average grayscale values of the three reference schemes are concurring, exactly equal to the half of the constant values.

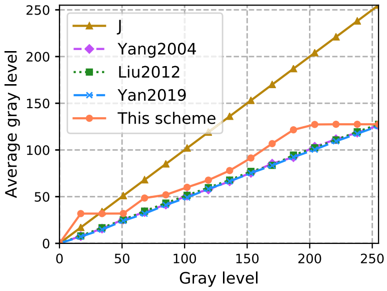

**FIGURE 8. Comparison of the average grayscale values.**

The local optimization strategy of the EDBS can largely simulate the tone of the original image. It can be found that the average grayscale value of the proposed scheme is higher than that of the reference schemes, and is also closer to the original image for each grayscale level. Therefore, the difference in brightness is verified both qualitatively and quantitatively.

### C. FIDELITY ANALYSIS

Two representative evaluation metrics, PSNR and MSSIM, are selected as the measurement indexes to analyze the fidelity of natural images in terms of image tone and image structure.

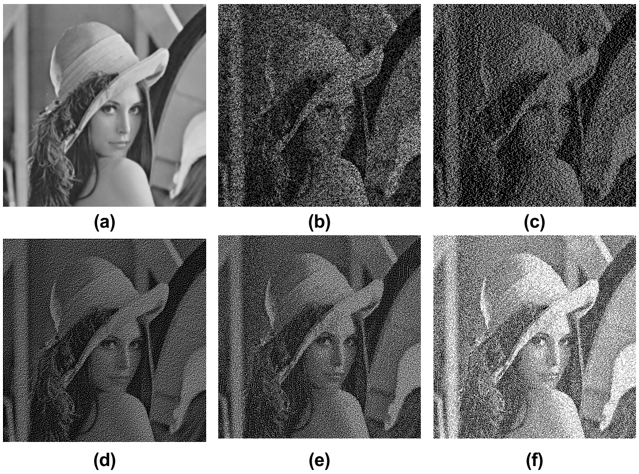
(a) (b) (c)

(d) (e) (f)

**FIGURE 9. Comparison of the reconstruction effect.**

Fig.9a shows the secret image, while Fig.9b, c, d, and e correspond to the superimposed results of the schemes proposed by Yang *et al.*, Liu *et al.*, Yan *et al.*, and this paper. Fig.9f is the image optimized by the information extracted from Fig.9e. The low-frequency band energy of Liu *et al.*'s. gradually declines with the increase of the grayscale value, while the probabilistic method is not improved. For the brighter area of Fig.9a, the distribution of minority pixels in Fig.9c is more uniform than that of Fig.9b. Therefore, the overall perception of Fig.9c is superior to Fig.9b. Based on the MEVC, Yan *et al.* employ the error diffusion technique to push the noise to the high-frequency band. Apart from the contrast reduction and color distortion caused by VC sharing, the presentation of Fig.9d possesses fair perceptual quality with evenly distributed minority pixels and fine structural features.

The display of this scheme is close to Yan *et al.*'s structure and detail presentation. Compared to Fig.9d, the brightness is higher in Fig.9e for the areas with higher local grayscale values, such as the front part of the hat. Thus, the overall contrast of the proposed scheme is higher than that of Yan *et al.*'s, which is also in line with the results in Fig.8. Therefore, the proposed scheme achieves good performance on tone and structure features and obtains a realistic presentation. Furthermore, the Fig.9f has enhanced contrast thanks to the information extraction, and is more approximate to the secret image in tone.

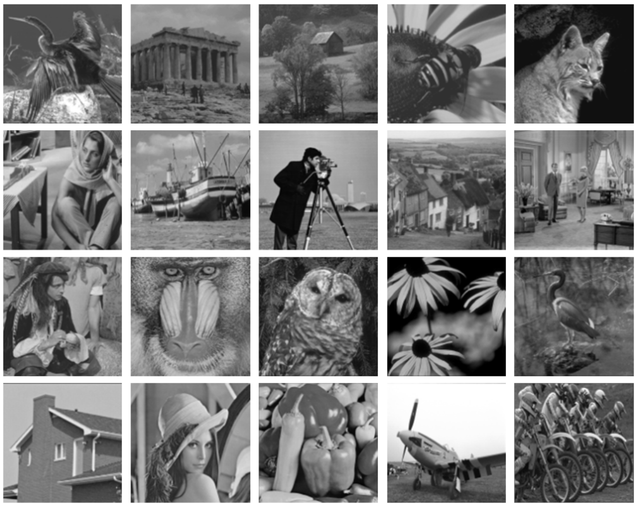

**FIGURE 10.** **The test atlas with a size of 512 × 512, indexed in a raster scanning order.**

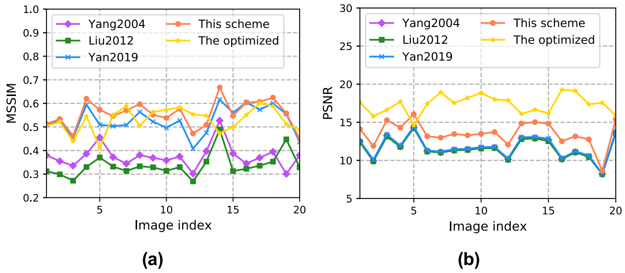

**FIGURE 11.** **Quantitative comparison on the test atlas.**

Based on the qualitative analysis above, we use the PSNR and MSSIM to quantify the comparison results in terms of tone and structural similarities. The test atlas shown in Fig.10 consists of 20 commonly used standard grayscale images indexed by the raster scanning order in the field of digital image processing. Fig.11a reveals that the structural similarity of Yan *et al.*'s and our proposed scheme are approximately similar, and the information extraction has no obvious impact on the structure improvement. By contrast, the performance of Yang *et al.* and Liu *et al.* is generally poor.

Fig.11b shows that the PSNR values of Yang *et al.*, Liu *et al.*, and Yan *et al.* are almost equal without an obvious difference, which is consistent with the results of the average grayscale value. The performance of the PSNR value of our scheme outperforms the reference schemes, i.e., the reconstructed image approximates to the secret image more. Furthermore, the optimized image is significantly improved in terms of contrast, and is closer to the grayscale secret image in tone. To sum up, the proposed scheme is superior to the reference schemes with regards to both tone and structure performance. Additionally, Fig.11 reveals that MSSIM is more effective than the PSNR in representing the perceptual effect of the reconstructed image. For the same MSSIM value, the higher the PSNR value is, the better the perceptual effect will be.

### D. COMPUTATIONAL COMPLEXITY

The time complexity of the proposed and the reference schemes are linear functions of the secret image size, i.e., $O(MN)$ with $M$ and $N$ denoting the row and column width of the grayscale secret image, which can be estimated by the number of basic operations or steps performed during algorithm execution.

Let the operation time of one addition/subtraction be $\mathcal{T}_{add}$, one multiplication/division be $\mathcal{T}_{\mathrm{mul}}$, and one random number generation be $\mathcal{T}_{rnd}$. The time complexity of Yan *et al.*'s scheme varies with different block size and the result is determined according to the current settings. Let the kernel size of PSF be $K$ and the total iterations of this scheme be $c$.

**TABLE 2.** **Comparison of Computational Complexion.**

| Operation<br>Scheme | $\mathcal{T}_{add}$ | $\mathcal{T}_{\mathrm{mul}}$ | $\mathcal{T}_{rnd}$ |
|---|---|---|---|
| Yang *et al.* [13] | error diffusion:<br>5*MN* | error diffusion:<br>4*MN* | sharing:<br>*MN* |
| Liu *et al.* [19] | error diffusion:<br>5*MN* | error diffusion:<br>4*MN* | sharing:<br>*MN* |
| Yan *et al.* [27] | Quantization:<br>2.25*MN*<br>error diffusion:<br>4.75 *MN* | gamut mapping:<br>*MN*<br>Quantization:<br>1.5*MN*<br>simulated superposition:<br>*MN*<br>error diffusion:<br>5.75*MN* | sharing:<br>*MN* |
| This scheme | error calculation:<br>*MN*<br>coefficient calculation:<br>2*KMN*<br>local optimization:<br>18*cMN*<br>coefficient adjustment:<br>2*cMN* | gamut mapping:<br>*MN*<br>simulated superposition:<br>(*c*+1) *MN*<br>local optimization:<br>72*cMN*<br>coefficient adjustment:<br>2*cMN* | sharing:<br>(*c*+1) *MN* |

The total time complexity of [13] and [19] is $5MN\mathcal{T}_{\mathrm{add}} + 4MN\mathcal{T}_{\mathrm{mul}} + MN\mathcal{T}_{\mathrm{rnd}}$ both. It is $7MN\mathcal{T}_{\mathrm{add}} + 9.25MN\mathcal{T}_{\mathrm{mul}} + MN\mathcal{T}_{\mathrm{rnd}}$ in [27] and $(75c+2)\,MN\mathcal{T}_{\mathrm{mul}} + (c+1)\,MN\mathcal{T}_{\mathrm{rnd}} + (20c+2K+1)MN\mathcal{T}_{\mathrm{add}})$ in this scheme. Table 2 discloses that the time complexity of our scheme is the highest among the reference schemes. For Lena image, the actual running time of [27] and this paper is respectively 1.87s and 8.13s on a laptop with Intel i7 CPU and 16GB memory.

## V. CONCLUSION

This paper proposes a structural model combining the MEVC sharing with the EDBS halftone technique for grayscale images to improve the perceptual quality of the reconstructed image, which nests the VC sharing into the EDBS optimization loop to guarantee the contrast and security conditions by the MEVC sharing and promote the perceptual quality by the EDBS. We also design an information extraction process to improve the contrast of the reconstructed image by the inverse mapping of the mapping relationship in the codebook.

The experiment and result analysis show that the minority pixels in the reconstructed image are uniformly distributed with visually-friendly observation, which conforms to the blue noise feature. The structure of the secret image is well recovered, the tone of the secret image is genuinely simulated, and the contrast of the reconstructed image is higher than the reference schemes. The information extraction process further enhances the contrast of the reconstructed image and produces an optimized image more similar to the secret image in terms of tone characteristics. The structural model of the proposed scheme has strong scalability; thus, it can be combined with other size-invariant methods, such as probabilistic VC and RG. In our future studies, we consider to integrate the multiple-level VC into the EDBS to generate a more exquisite presentation of the reconstructed image.

## ACKNOWLEDGMENT

The authors would like to thank the editor and the anonymous reviewers for their valuable suggestions and comments.

## REFERENCES

[1] M. Naor and A. Shamir, "Visual cryptography," in *Proc. Workshop Theory Appl. Cryptogr. Techn. (EUROCRYPT)*, Perugia, Italy, 1994, pp. 1–12.

[2] S. Droste, "New results on visual cryptography," in *Advances in Cryptology—CRYPTO'96* (Lecture Notes in Computer Science), vol. 1109, N. Koblitz, Ed. Berlin, Germany: Springer, 1996, pp. 401–415, 1996, doi: 10.1007/3-540-68697-5_30.

[3] C. Blundo, S. Cimato, and A. De Santis, "Visual cryptography schemes with optimal pixel expansion," *Theor. Comput. Sci.*, vol. 369, nos. 1–3, pp. 169–182, Dec. 2006, doi: 10.1016/j.tcs.2006.08.008.

[4] F. Liu, C. Wu, and X. Lin, "Step construction of visual cryptography schemes," *IEEE Trans. Inf. Forensics Security*, vol. 5, no. 1, pp. 27–38, Mar. 2010, doi: 10.1109/TIFS.2009.2037660.

[5] R. Lakshmanan and S. Arumugam, "Construction of a (k, n)-visual cryptography scheme," *Des., Codes Cryptogr.*, vol. 82, no. 3, pp. 629–645, Mar. 2017, doi: 10.1007/s10623-016-0181-z.

[6] T. Guo, J. Jiao, F. Liu, and W. Wang, "On the pixel expansion of visual cryptography scheme," *Int. J. Digit. Crime Forensics*, vol. 9, no. 2, pp. 38–44, Apr. 2017, doi: 10.4018/IJDCF.2017040104.

[7] O. Kafri and E. Keren, "Encryption of pictures and shapes by random grids," *Opt. Lett.*, vol. 12, no. 6, pp. 377–379, 1987, doi: 10.1364/OL.12.000377.

[8] T.-H. Chen and K.-H. Tsao, "Threshold visual secret sharing by random grids," *J. Syst. Softw.*, vol. 84, no. 7, pp. 1197–1208, Jul. 2011, doi: 10.1016/j.jss.2011.02.023.

[9] X. Wu and W. Sun, "Improving the visual quality of random grid-based visual secret sharing," *Signal Process.*, vol. 93, no. 5, pp. 977–995, May 2013, doi: 10.1016/j.sigpro.2012.11.014.

[10] H. Hu, G. Shen, Z. X. Fu, and B. Yu, "Improved contrast for threshold random-grid-based visual cryptography," *KSII Trans. Internet Inf. Syst.*, vol. 12, no. 7, pp. 3401–3420, 2018, doi: 10.3837/tiis.2018.07.022.

[11] X. Wu and Z.-R. Lai, "Random grid based color visual cryptography scheme for black and white secret images with general access structures," *Signal Process., Image Commun.*, vol. 75, pp. 100–110, Jul. 2019, doi: 10.1016/j.image.2019.03.017.

[12] R. Ito, H. Kuwakado, and H. Tanaka, "Image size invariant visual cryptography," *IEICE Trans. Fundam.*, vol. 82, no. 10, pp. 2172–2177, Oct. 1999, doi: 10.1109/98.799622.

[13] C.-N. Yang, "New visual secret sharing schemes using probabilistic method," *Pattern Recognit. Lett.*, vol. 25, no. 4, pp. 481–494, Mar. 2004, doi: 10.1016/j.patrec.2003.12.011.

[14] Y. C. Hou, Z. Y. Quan, and C. F. Tsai, "Progressive visual cryptography with friendly and size invariant shares," *Int. Arab J. Inf. Technol.*, vol. 15, no. 2, pp. 321–330, 2018.

[15] X. Wu and C.-N. Yang, "Probabilistic color visual cryptography schemes for black and white secret images," *J. Vis. Commun. Image Represent.*, vol. 70, Jul. 2020, Art. no. 102793, doi: 10.1016/j.jvcir.2020.102793.

[16] C.-N. Yang, C.-C. Wu, and D.-S. Wang, "A discussion on the relationship between probabilistic visual cryptography and random grid," *Inf. Sci.*, vol. 278, pp. 141–173, Sep. 2014, doi: 10.1016/j.ins.2014.03.033.

[17] Y. C. Hou and C. F. Tu, "Visual cryptography techniques for color images without pixel expansion," (in Chinese), *J. Inf., Technol. Soc.*, vol. 1, pp. 95–110, Jun. 2004.

[18] Y. C. Hou and S. F. Tu, "A visual cryptographic technique for chromatic images using multi-pixel encoding method," *J. Res. Pract. Inf. Technol.*, vol. 37, no. 2, pp. 179–191, 2005, doi: 10.1007/s10851-005-4897-z.

[19] F. Liu, T. Guo, C. Wu, and L. Qian, "Improving the visual quality of size invariant visual cryptography scheme," *J. Vis. Commun. Image Represent.*, vol. 23, no. 2, pp. 331–342, Feb. 2012, doi: 10.1016/j.jvcir.2011.11.003.

[20] H. Zhang, X. Wang, and Y. Huang, "Secret image sharing based on self-adaptive multi-pixel encoding," (in Chinese), *J. Southwest Jiaotong Univ.*, vol. 44, no. 3, pp. 448–454, 2009.

[21] Y.-F. Chen, Y.-K. Chan, C.-C. Huang, M.-H. Tsai, and Y.-P. Chu, "A multiple-level visual secret-sharing scheme without image size expansion," *Inf. Sci.*, vol. 177, no. 21, pp. 4696–4710, Nov. 2007, doi: 10.1016/j.ins.2007.05.011.

[22] C.-C. Lee, H.-H. Chen, H.-T. Liu, G.-W. Chen, and C.-S. Tsai, "A new visual cryptography with multi-level encoding," *J. Vis. Lang. Comput.*, vol. 25, no. 3, pp. 243–250, Jun. 2014, doi: 10.1016/j.jvlc.2013.11.001.

[23] Z. Zhou, G. R. Arce, and G. Di Crescenzo, "Halftone visual cryptography," *IEEE Trans. Image Process.*, vol. 15, no. 8, pp. 2441–2453, Aug. 2006.

[24] Z. Wang, G. R. Arce, and G. D. Crescenzo, "Halftone visual cryptography via direct binary search," in *Proc. Eur. Signal Process. Conf. (Eusipco)*, Sep. 2006, pp. 1–5.

[25] X. Yan, S. Wang, X. Niu, and C.-N. Yang, "Halftone visual cryptography with minimum auxiliary black pixels and uniform image quality," *Digit. Signal Process.*, vol. 38, pp. 53–65, Mar. 2015, doi: 10.1016/j.dsp.2014.12.002.

[26] M. E. Hodeish and V. T. Humbe, "An optimized halftone visual cryptography scheme using error diffusion," *Multimedia Tools Appl.*, vol. 77, no. 19, pp. 24937–24953, Oct. 2018, doi: 10.1007/s11042-018-5724-z.

[27] B. Yan, Y. Xiang, and G. Hua, "Improving the visual quality of size-invariant visual cryptography for grayscale images: An analysis-by-synthesis (AbS) approach," *IEEE Trans. Image Process.*, vol. 28, no. 2, pp. 896–911, Feb. 2019, doi: 10.1109/TIP.2018.2874378.

[28] M. Analoui and J. P. Allebach, "Model based halftoning using direct binary search," *Proc. SPIE*, vol. 1666, pp. 96–108, Aug. 1992, doi: 10.1117/12.135959.

[29] Z. Wang, E. P. Simoncelli, and A. C. Bovik, "Multiscale structural similarity for image quality assessment," in *Proc. 37th Asilomar Conf. Signals, Syst. Comput.*, vol. 2, Nov. 2003, pp. 1398–1402, doi: 10.1109/ACSSC.2003.1292216.

[30] F. A. Baqai and J. P. Allebach, "Halftoning via direct binary search using analytical and stochastic printer models," *IEEE Trans. Image Process.*, vol. 12, no. 1, pp. 1–15, Jan. 2003, doi: 10.1109/TIP.2002.806244.

[31] D. L. Lau and G. R. Arce, *Modern Digital Halftoning*, 2nd ed. Boca Raton, FL, USA: CRC Press, 2008.

[32] Z. Wang, A. C. Bovik, H. R. Sheikh, and E. P. Simoncelli, "Image quality assessment: From error visibility to structural similarity," *IEEE Trans. Image Process.*, vol. 13, no. 4, pp. 600–612, Apr. 2004.

**RUI SUN** received the B.S. degree in information engineering, in 2013. He is currently pursuing the master's degree with the Zhengzhou Information Science and Technology Institute. His research interests include visual cryptography and information security.

**ZHENGXIN FU** received the M.S. and Ph.D. degrees from the Zhengzhou Information Science and Technology Institute, in 2010 and 2014, respectively. His research interests include visual cryptography and information security.

**BIN YU** received the B.S. degree from the Department of Electronic Engineering, Shanghai Jiao Tong University, in 1986, the M.S. degree from the Department of Automatic Engineering, South China University of Technology, in 1991, and the Ph.D. degree, in 1999. He worked as a Research Assistant with The Hong Kong University of Science and Technology. From 2003 to 2004, he worked as a Vice Professor with the University of Waterloo, Waterloo, ON, Canada. He is currently a Professor with the Department of Computer Science and Information Engineering, Zhengzhou Information Science and Technology Institute, China. His research interests include the design and analysis of algorithms, visual secret sharing, and network security.